Parallel simulations of Hall MHD plasmas

Daniel Gómez[1,2]
(1) Instituto de Astronomía y Física del Espacio (IAFE), Buenos Aires, Argentina
(2) Department of Physics, University of Buenos Aires, Buenos Aires, Argentina

October 28, 2005

Abstract. Plasma processes such as magnetic reconnection, turbulent regimes or dynamo-generated magnetic fields, are well studied within the framework of one-fluid magnetohydrodynamics (MHD). However, there are processes such as the Hall current, which are not covered by the MHD description. The Hall effect is known to be relevant for the dynamics of several astrophysical plasmas, such as the interstellar medium, the early universe, or the solar wind at 1 AU. While the relevance of Hall currents in magnetic reconnection is intensively being studied (specially in connection with reconnection events at the Earth's magnetopause and magnetotail), their role on turbulent regimes or on dynamo mechanisms is mostly unknown. We report results from parallel simulations of the incompressible Hall MHD equations in $2\frac{1}{2}$ and three dimensions to quantitatively investigate the role of Hall currents in different problems, such as magnetic reconnection in $2\frac{1}{2}$ dimensions, the dynamo generation of magnetic fields in three dimensional simulations, or the relaxation to stationary turbulent regimes.

Keywords: MHD, turbulence, MHD dynamo, magnetic reconnection

1. Introduction

Numerical simulations have become an important tool for fluid mechanics in recent years. The large-scale dynamics of plasma flows can often be described within a fluidistic approximation known as one-fluid magnetohydrodynamics. Complex flows such as those corresponding to turbulent regimes are ubiquitous in laboratory plasmas and in astrophysics, because of their typically very large Reynolds numbers.

Hall currents can in turn play a significant role in the dynamics of low density and/or low temperature astrophysical plasmas, for which a one fluid description has been traditionally used. For instance, they are likely to be relevant in dense molecular clouds (Wardle and Ng, 1999), accretion disks (Balbus and Terquem, 2001; Sano and Stone, 2002), white dwarfs and neutron stars (Yakovlev and Urpin, 1980), and the early universe (Tajima et al., 1992).

Magnetic reconnection is likely to be the main mechanism by which the energy stored in stressed magnetic fields can be converted into kinetic and thermal energy. It is believed to play a crucial role in different astrophysical environments such as the Earth's magnetopause (Sonnerup et al., 1981), the Earth's magnetotail (Birn and Hesse, 1996)

or the solar atmosphere (Priest, 1984). In recent years many analytical and computational efforts have been made to clarify the importance of the Hall effect in the reconnection process (Birn et al., 2001; Craig and Watson, 2003; Dorelli and Birn, 2003; Dorelli, 2003; Smith et al., 2004). Also, observed signatures of these Hall currents have been reported (Mozer, Bale and Phan, 2002).

One of the interesting features of the Hall-MHD description, is that in the ideal limit (i.e. without resistivity) the magnetic field is stretched by the electron velocity field rather than the bulk velocity field. Since these two velocity fields can be quite different, the Hall term is expected to impact on dynamo mechanisms. The Hall term was found (Mininni, Gómez and Mahajan, 2002) to enhance or suppress dynamo action depending on the relative importance of the Hall term when compared to the inductive term. We perform 3D numerical simulations of the Hall-MHD equations to explore the role of the Hall current in the efficiency of the dynamo.

In Section 2 we describe the so-called Hall-MHD equations, which stem from a two-fluid description of the plasma. In Section 3 we study the importance of the Hall term in magnetic reconnection, by performing numerical simulations of an incompressible $2\frac{1}{2}$D Hall-MHD code. In Section 4 we present the results from 3D simulations of the Hall-MHD equations, which started from a weak magnetic seed to study the role of the Hall current in the efficiency of a turbulent dynamo. Finally, in Section 5 we list our conclusions.

2. The Hall-MHD equations

Highly conductive plasmas tend to develop thin and intense current sheets in their reconnection layers. Whenever the current width reaches values as low as c/w_{pi} (w_{pi} is the ion plasma frequency and c is the speed of light), it is no longer possible to neglect the Hall term in Ohm's law (Ma and Bhattacharjee, 2001). For a fully ionized plasma of protons and electrons, the generalized Ohm's law can be written as:

$$\boldsymbol{E} + \frac{1}{c}\boldsymbol{v} \times \boldsymbol{B} = \frac{1}{\sigma}\,\boldsymbol{j} + \frac{1}{ne}\,(\frac{1}{c}\boldsymbol{j} \times \boldsymbol{B} \;-\; \nabla p_e)\;, \tag{1}$$

where n is the electron and proton density, e is the electron charge, σ is the electric conductivity, $\boldsymbol{v}$ is the plasma flow velocity, and $\boldsymbol{j}$ is the electric current density. Assuming incompressibility (i.e. $\nabla \cdot \boldsymbol{v} = 0$), the Hall-MHD equations can be cast in their dimensionless form as:

$$\partial_t \boldsymbol{v} + (\boldsymbol{v} \cdot \nabla)\boldsymbol{v} = (\nabla \times \boldsymbol{B}) \times \boldsymbol{B} - \nabla p + \nu \nabla^2 \boldsymbol{v}\;, \tag{2}$$

$$\partial_t \boldsymbol{B} = \nabla \times [(\boldsymbol{v} - \epsilon \nabla \times \boldsymbol{B}) \times \boldsymbol{B}] + \eta \nabla^2 \boldsymbol{B} \ , \tag{3}$$

$$\nabla \cdot \boldsymbol{B} = 0 = \nabla \cdot \boldsymbol{U} \ . \tag{4}$$

In equations (2)-(4) we have normalized $\boldsymbol{B}$ and $\boldsymbol{v}$ to the Alfvén speed $v_a = B_0/\sqrt{4\pi\rho}$ (B_0: magnetic field intensity, ρ: mass density), the total gas pressure p to ρv_a^2, and longitudes and times respectively to L_0 and L_0/v_a. The dimensionless dissipation coefficients are the viscosity ν and the electric resistivity η defined as $\eta = c^2/(4\pi\sigma L_0 v_a)$. The dimensionless coefficient $\epsilon = c/(w_{pi}\ L_0)$ is a measure of the relative strength of the Hall effect. The dimensionless electron velocity is:

$$\boldsymbol{v_e} = \boldsymbol{v} - \epsilon \nabla \times \boldsymbol{B} \ . \tag{5}$$

From equation (3) it is apparent that in the non-dissipative limit (i.e. $\eta \to 0$) the magnetic field remains frozen to the electron flow $\boldsymbol{v_e}$ rather than to the bulk velocity $\boldsymbol{v}$.

3. Simulations of Hall-reconnection

The incompressible Hall MHD simulations reported in this paper are carried out under the geometric approximation known as $2\frac{1}{2}$D, based on the assumption that there is translational symmetry along the $\hat{\boldsymbol{z}}$ coordinate (i.e. $\partial_z = 0$). Therefore, the solenoidal magnetic and velocity fields can be represented as:

$$\boldsymbol{B} = \nabla \times [\hat{\boldsymbol{z}} a(x,y,t)] + \hat{\boldsymbol{z}} b(x,y,t) \ , \tag{6}$$

$$\boldsymbol{U} = \nabla \times [\hat{\boldsymbol{z}} \phi(x,y,t)] + \hat{\boldsymbol{z}} u(x,y,t) \ , \tag{7}$$

where $a(x,y,t)$ is the magnetic flux function and $\phi(x,y,t)$ is the stream function. In this approximation, the Hall MHD equations take the form:

$$\partial_t a = [\phi - \epsilon b, a] + \eta \nabla^2 a \ , \tag{8}$$

$$\partial_t b = [\phi, b] + [u - \epsilon j, a] + \eta \nabla^2 b \ , \tag{9}$$

$$\partial_t w = [\phi, w] + [j, a] + \nu \nabla^2 w \ , \tag{10}$$

$$\partial_t u = [b, a] + [\phi, u] + \nu \nabla^2 u \ . \tag{11}$$

The nonlinear terms are the standard Poisson brackets, $w = -\nabla^2 \phi$ is the $\hat{\boldsymbol{z}}$-component of the flow vorticity and $j = -\nabla^2 a$ is the $\hat{\boldsymbol{z}}$-component of the electric current density

$$\boldsymbol{j} = \nabla \times b\, \hat{\mathbf{z}} + j\, \hat{\mathbf{z}} \tag{12}$$

The set of Equations (8)-(11) completely describe the reconnection problem for this particular geometry.

One of the most important consequences of including the Hall effect is the coupling between the $\hat{\boldsymbol{z}}$-component of the fields to the scalar potentials a and ϕ. Note that if $\epsilon = 0$, then the system decouples and the solutions for a and ϕ are determined by the solution of equations (8) and (10), thus becoming completely independent from the $\hat{\boldsymbol{z}}$ fields.

We study Hall reconnection by means of the numerical integration of Equations (8)-(11). The computation is carried out in a rectangular domain assuming periodic boundary conditions. The fields are expanded in their corresponding spatial Fourier amplitudes. The equations for these Fourier amplitudes are evolved in time using a second order Runge-Kutta scheme and the nonlinear terms are evaluated following a 2/3 dealiased pseudospectral technique. To provide a reconnection scenario, the simulations start with the fluid at rest, and the following initial condition for the $\hat{\boldsymbol{y}}$ component of the magnetic field:

$$\boldsymbol{B}_y(x, y, t = 0) = \begin{cases} B_0 \tanh[\frac{x-\pi/2}{\Delta}] & \text{if } -\pi \leq x < 0 \\ \\ -B_0 \tanh[\frac{x+\pi/2}{\Delta}] & \text{if } 0 \leq x < \pi \end{cases} \tag{13}$$

corresponding to a periodic array of oppositely oriented current sheets. In the present paper we chose $B_0 = 1$ and $\Delta = 0.04\pi$, to simulate two initially thin current sheets, where the reconnection process will take place. In order to drive reconnection, a monocromatic perturbation with $k_x = 1$ and an amplitude of 2% of the initial magnetic profile (see Equation (13)) is added to the initial condition in the full rectangular domain. We performed numerical simulations with a spatial resolution of 512×512 grid points, and different values of the Hall parameter ϵ to study the role of the Hall term in the overall dynamics of the reconnection process. In all these simulations, the dissipation coefficients are set to $\eta = \nu = 0.01$ to ensure that all the lengthscales are properly resolved. Note that pseudospectral methods conserve the energy of the system, i.e. no numerical dissipation is artificially introduced by the simulation (Canuto et al., 1988).

Figure 1 shows the regions where the electric current density surpasses 30% of its maximum value for the whole run. For this particular run ($\epsilon = 0.07$), the maximum current ($j_{max} = 10.5$) was attained at $t \approx 1$, which corresponds to the left frame. The central and right frames correspond to $t = 2, 3$ respectively. White (black) regions correspond to positive (negative) currents. It can be readily seen that the current sheet becomes shorter and thinner and resembles a structure of the type suggested by Petschek (although the physics is quite different). This shortening and shrinkage of the current sheet comes along with the

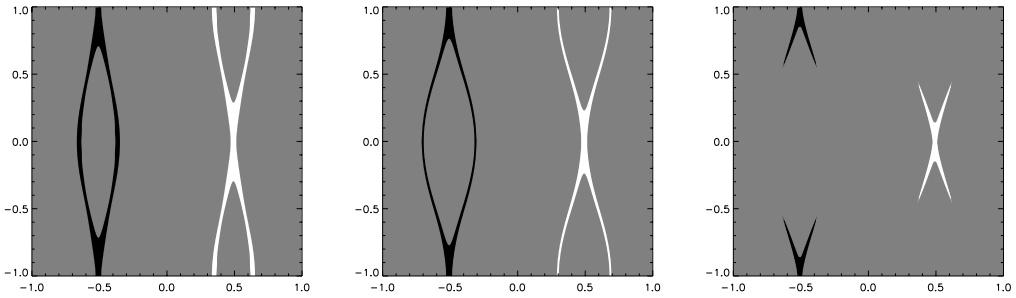

Figure 1. Current density spatial distribution. White (black) regions correspond to current densities surpassing 30% of the maximum positive (negative) value.

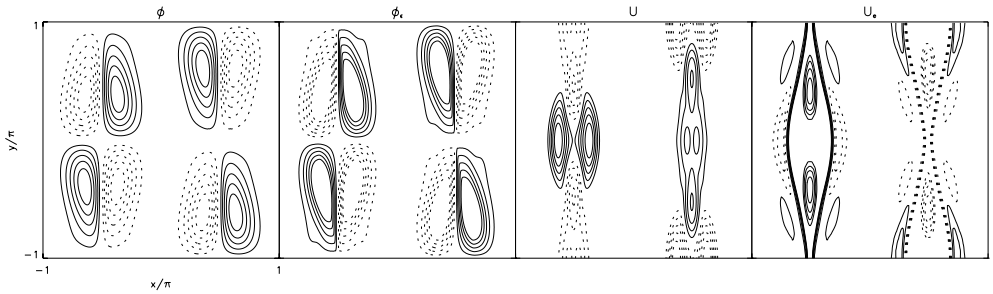

Figure 2. The first two panels display stream function contour plots for protons (ϕ) and electrons (ϕ_e) during maximal reconnection rate ($t = 1$). The last two panels show the corresponding out-of-plane velocities.

development of a quadrupolar structure of the out-of-plane magnetic field component around the X-points (Sonnerup et al., 1981).

The first two panels of Figure 2 show contour plots of the proton (ϕ) and electron (ϕ_e) stream functions at $t = 1$. The difference between these patterns contributes to the in-plane current density, which in turn generates the out-of-plane magnetic field (first term on the RHS of equation (12)). The two right hand panels in Figure 2 show contours of the out-of-plane velocities of protons (u) and electrons (u_e). The two species show entirely different velocity patterns. Note that in the ideal limit the magnetic field remains frozen to the electron flow, which is faster than the proton flow.

One of the most important features to evaluate the efficiency of the reconnection process is the reconnected flux. The magnetic flux reconnected as a function of time at the X point can be calculated in terms of the difference of the magnetic potential in the X-point and the O-point, i.e. $a_X(t) - a_O(t)$. The effect of the Hall term on the reconnected flux is shown in Figure 3. As ϵ is increased the reconnection

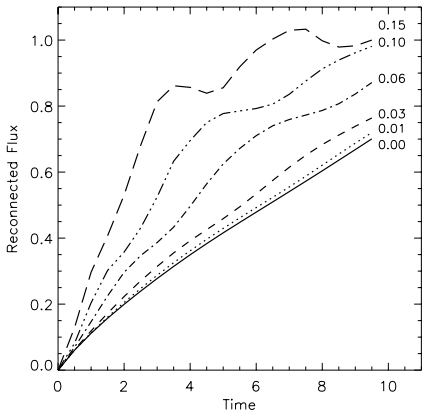

Figure 3. Total reconnected magnetic flux vs. time, for simulations with different values (indicated) of ϵ.

process is observed to become more efficient, as evidenced by the total reconnected flux.

4. Simulations of Hall-dynamos

We developed a pseudospectral code (see details in (Mininni, Gómez and Mahajan, 2003)), which was modified to run in a Beowulf cluster using MPI (Message Passing Interface). We integrated the Hall-MHD equations (2)-(4) in a cubic box with periodic boundary conditions. The equations were evolved using a second order Runge-Kutta method. The total pressure $P_T = P + B^2/2$ was computed in a self-consistent fashion at each time step to ensure the incompressibility condition $\nabla \cdot \boldsymbol{U} = 0$ (Canuto et al., 1988). To satisfy the divergence-free condition for the magnetic field, equation (3) was replaced by an equation for the vector potential $\boldsymbol{A}$, and the electron pressure p_e was computed at each time step to satisfy the Coulomb gauge $\nabla \cdot \boldsymbol{A} = 0$.

The relevance of the Hall term on dynamo activity was explored in a previous paper (Mininni, Gómez and Mahajan, 2003). Our simulations are performed in two stages: (1) a purely kinetic stage (the magnetic field is zero) during which we externally drive the fluid with a helical force until a Kolmogorov turbulent regime is reached, (2) we implant a mild magnetic fluctuation (or seed) at microscopic scales and restart the externally driven run. The (inititally very small) magnetic energy grows exponentially fast during a kinematic dynamo regime and then it saturates at a level of approximate equipartition between kinetic and magnetic energy. Figure 4 (left) shows the spatial distribution of

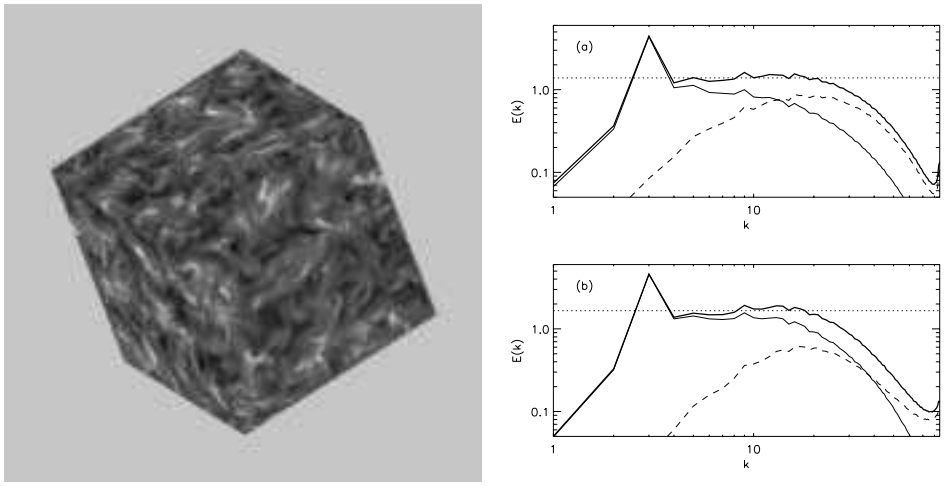

Figure 4. Left: Three dimensional Hall-MHD simulation with 256^3 gridpoints showing the spatial distribution of magnetic energy in the saturated regime. Right: Total compensated energy spectrum (thick trace), kinetic energy spectrum (thin trace) and magnetic energy spectrum (dashed) for runs with (a) $\epsilon = 0$ and (b) $\epsilon = 0.1$.

magnetic energy for a 256^3 simulation with $\epsilon = 0.1$ during the saturated regime.

The saturation amplitude of the Hall-MHD dynamo has a nonlinear dependence with the amplitude of the Hall effect. When the Hall length-scale is close to or smaller than the Kolmogorov's magnetic dissipation scale, the MHD behavior is recovered ($\epsilon \ll 1$) and no differences in the evolution and saturation of the dynamo can be identified. On the other hand, when the Hall effect dominates in all the relevant scales including the energy containing scales of the turbulent flow ($\epsilon \approx 1$), the helical dynamo is less efficient than its MHD counterpart. The dynamo saturates at a lower level of total magnetic energy, and the kinetic energy dominates the dynamics at almost all scales. However, there is an intermediate regime in which the dynamo effect is enhanced by the Hall term. In this regime, the Hall effect dominates the dynamics at intermediate scales up to the diffusion scale.

One interesting result is the fact that the energy power spectrum for a turbulent Hall dynamo, shows a Kolmogorov slope. In Figure 4 (right) we show compensated power spectra, i.e. $k^{5/3}\epsilon^{-2/3}E_k$ vs. k, both for a purely MHD run ($\epsilon = 0$, above) and for Hall-MHD ($\epsilon = 0.1$, below). Even though some differences can be observed (for instance, an excess of magnetic energy at small scales for the MHD case), the Kolmogorov slope remains esentially unaffected when the Hall effect is considered.

5. Conclusions

We have investigated the role of the Hall effect in two astronomically relevant plasma processes: magnetic reconnection and turbulent dynamos. With this goal in mind, we performed numerical simulations of the incompressible Hall-MHD equations in $2\frac{1}{2}$D and 3D using a pseudospectral scheme.

For the $2\frac{1}{2}$D magnetic reconnection runs, we confirm the global scenario described by previous authors, such as the development of smaller and thinner current sheets, the formation of a quadrupolar structure in the out-of-plane magnetic field component, and the generation of out-of-plane flows in the surroundings of the X-points. More importantly, we confirm that the Hall effect leads to a faster reconnection process, as evidenced by the larger total reconnected flux.

In our 3D simulations of a turbulent Hall dynamo, we find that the Hall current modifies the dynamo efficiency. Whenever the Hall lengthscale remains smaller than the energy containing scale but much larger than the dissipation scale, the magnetic energy saturates at a level higher than its MHD counterpart. Also, in the saturated regime, the energy power spectrum of this Hall-MHD turbulence displays a Kolmogorov slope, such as for pure MHD.

References

Balbus, S.A. & Terquem, C. *Astrophys. J.*, 552:235, 2001.
Birn, J et al. *J. Geophys. Res.*, 106:3715-19, 2001.
Birn, J. & Hesse, M., J. *J. Geophys. Res.*, 101:15345-58, 1996.
Canuto, C., Hussaini, M.Y., Quarteroni, A., & Zang, T.A. *"Spectral Methods in Fluid Dynamics"*, Springer-New York, 1988.
Craig, I.J.D., & Watson, P.G. *Solar Phys*, 214:130-150, 2003.
Dorelli, J. C. *Phys. Plasmas*, 10:3310-3314, 2003.
Dorelli, J. C. & Birn, J. *J. Geophys. Res.*, 108:1133, 2003.
Ma, Z & Bhattacharjee, A. *J. Geophys. Res.*, 106:3773, 2001.
Mininni, P. D., Gómez, D. O., & Mahajan, S. M. *Astrophys. J. Lett.*, 81–83, 2002.
Mininni, P.D., Gómez, D.O., & Mahajan, S.M. *Astrophys. J.*, 587:472-481, 2003.
Mozer, F., Bale, S., Phan, T. D. *Phys. Rev. Lett.*, 89:015002, 2002.
Priest, E. R. in "Magnetic Reconnection in Space and Laboratory Plasmas", edited by E. W. Hones (Washington, D. C.) *Geophys. Monogr. Ser.*, 30:63, 1984.
Sano, T. & Stone, J.M. *Astrophys. J.*, 570:314, 2002.
Smith, D., Ghosh, S., Dmitruk, P., & Matthaeus, W.H. *Geophys. Res. Lett.*, 31:L02805, 2004.
Sonnerup, B.U.O. et al. *J. Geophys. Res.*, 86:10049, 1981.
Tajima, T., Cable, S., Shibata, K., & Kulsrud, R. M. *Astrophys. J.*, 390:309-321, 1992.
Wardle, M., & Ng, C. *Mon. Not. R.A.S.*, 303:239-246, 1999.
Yakovlev, D. G. & Urpin, V. A. *Astr. Zh.*, 57:526–536, 1980.